Tunneling Cyclotron Resonance and the Renormalized Effective Mass in Semiconductor Barriers

G. Brozak
Physics Department, Northeastern University, Boston, Massachusetts 02115

E. A. de Andrada e Silva and L. J. Sham
Physics Department, University of California, San Diego, La Jolla, California 92093

F. DeRosa, P. Miceli, S. A. Schwarz, J. P. Harbison, L. T. Florez, and S. J. Allen, Jr.
Bellcore, Red Bank, New Jersey 07701
(Received 5 September 1989)

Tunneling cyclotron resonance is used to measure the tunneling rate deep in the band gap of a pure AlAs barrier in a thin barrier GaAs/AlAs superlattice. The experimental results are analyzed in terms of a four-band $\mathbf{k}\cdot\mathbf{P}$ model which leads to a renormalized effective mass in the barrier. Excellent agreement with experiment is achieved and we are able to conclude that the mass in the AlAs barrier is strongly renormalized down to $0.09m_e$ from the bulk-conduction-band value of $0.15m_e$.

PACS numbers: 73.40.Gk, 71.25.Jd

Semiconductor barrier transport is the controlling element in novel transport physics in a wide variety of semiconductor heterostructures and superlattices (SL's). For the most part semiconductor barrier tunneling is modeled in terms of an effective-mass approximation, with a modest attempt to recognize the real attributes of the barrier by choosing the appropriate band mass for the barrier.[1] In fact, tunneling usually takes place at an energy well below the barrier conduction-band edge so that the use of the band-edge barrier effective mass is extremely suspect and the real band structure[2] of the barrier[3,4] should be recognized.

Archetypical AlAs barriers in GaAs are a case in point. The Γ-point barrier is approximately 1 eV high, so Γ-point electrons tunneling from GaAs access states far from the corresponding AlAs band edge, deep in the gap, which are not properly described by the AlAs conduction-band Γ point. Recently, the extensive treatment by Moore *et al.*[5] indicates that the optical properties are accounted for by Bastard's[3] implementation of the Kane model[2] which attempts to realistically treat electron states in the wells and barriers far from the respective band edges. Although the agreement is quite good, the optical data, burdened by excitonic shifts, do not have the sensitivity to accurately determine the decay rate of the evanescent states in the barrier.

Here we report the first quantitative measurements of the tunneling rate deep in the forbidden energy gap of pure AlAs barriers. These results were obtained via tunneling cyclotron resonance measurements, which are sensitive, specific, and quantitative probes of coherent barrier transport. The experimental results are analyzed and compared with the predictions of a four-band $\mathbf{k}\cdot\mathbf{P}$ model. Excellent agreement is achieved and we are able to conclude that the X point plays no role in coherent barrier transport here and that the tunneling electron may be described by Γ electrons with a mass strongly renormalized from the AlAs band-edge value of $0.15m_e$ down to $0.09m_e$.[6,7]

The sample consists of 625 repetitions of SL period grown by molecular-beam epitaxy on a (100) oriented semi-insulating GaAs substrate. The period of the sample was accurately determined by x-ray diffraction to be 84.4 ± 0.1 Å; secondary-ion mass spectroscopy was used to measure the average Al concentration in the sample allowing us to infer a barrier width of 10.5 ± 0.6 Å.[8] Throughout the growth process Si donors were incorporated at a low doping density of 2×10^{15} cm^{-3} in order to minimize the density of scattering centers. In performing cyclotron resonance (CR) measurements we used a slow scan far-infrared Fourier-transform spectrometer in conjunction with a 15-T superconducting magnet. The cyclotron resonance was observed as an absorption in the far-infrared transmission spectrum at fixed magnetic fields. Because the density of carriers in this sample is low, the CR absorption is very weak. We increase the sensitivity of the CR measurement by modulating the carrier density in the SL. Crude field-effect transistors were made from the SL samples as described by Duffield *et al.*[9] The fractional change in transmission was measured as the samples were modulated between the approximately unperturbed (e.g., flat-band) condition to the condition where all the carriers are depleted from the SL layers. In addition, all the measurements were performed at 75 K in order to ensure that the majority of donors are ionized.

Figure 1 shows the experimental tunneling CR absorption spectra. At low fields, where the cyclotron energy is well within the SL subband width, the linewidths are relatively sharp reflecting the fact that the lower-lying magnetic levels show little dispersion along the growth axis.[9-12] At higher fields, as the CR energy approaches the miniband width, the magnetic levels develop strong dispersion along the growth axis, and the absorption

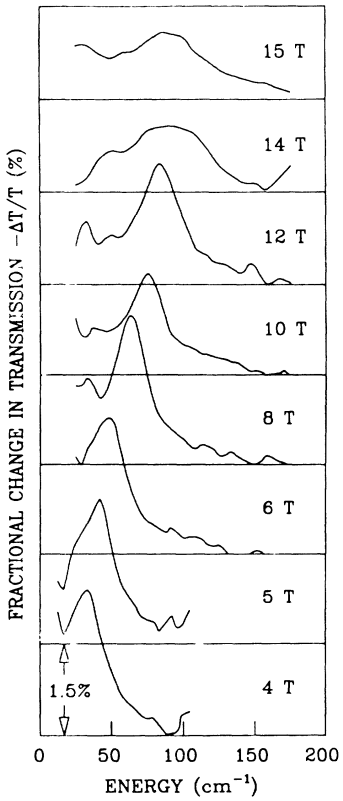

FIG. 1. Tunneling cyclotron resonance absorption spectra obtained with the magnetic field oriented perpendicular to the growth direction and at a temperature of 75 K.

tends to broaden and saturate. This is discussed in more detail below.

A simple estimate, using the Kronig-Penney model, shows that the first subband of the X profile with wells in AlAs lies more than 150 meV above the first Γ-profile subband so that the Γ-X interaction may be neglected.[13] We adopt a four-band $\mathbf{k}\cdot\mathbf{P}$ model for the Γ profile in both the GaAs wells and the AlAs barriers.[2-4] For tunneling CR the growth axis of the superlattice is taken to be along the z axis and the magnetic field $\mathbf{B}$ is along the x axis which in the Landau gauge leads to a vector potential $\mathbf{A}=B(0,-z,0)$. The period L of the superlattice is equal to the sum of the well thickness L_w and barrier thickness L_b. With the field in this configuration the position of the CR orbit center along the growth axis R_z is a good quantum number and the magnetic subbands can be characterized in terms of two quantum numbers which are components of a two-dimensional wave vector (k_x,k_y),[14] where $R_z=k_y l^2$, and $l=(\hbar/eB)^{1/2}$ is the magnetic length.

With the neglect of the spin-orbit interaction in the four-band model, the wave function is of the form

$$\psi=\sum F_i u_i, \quad i=S,P_x,P_y,P_z, \tag{1}$$

where $\{u_i\}$ is the basis of Bloch waves of the bulk-conduction and valence bands at the Γ point and F_i are the corresponding envelope functions. The basis functions u_i and the momentum matrix elements between the conduction- and valence-band states P are taken to be the same in both materials in order to preserve flux conservation across the interface.[4] The envelope functions are of the form

$$F_i=f_i(z)\exp(ik_x x+ik_y y) \tag{2}$$

and, neglecting the quadratic terms in k, the eigenenergies are given by

$$\begin{pmatrix} V+\Delta-E & Pk_x & P(k_y-z/l^2) & -iP\,d/dz \\ Pk_x & V-\Delta-E & 0 & 0 \\ P(k_y-z/l^2) & 0 & V-\Delta-E & 0 \\ -iP\,d/dz & 0 & 0 & V-\Delta-E \end{pmatrix} \begin{pmatrix} f_s \\ f_x \\ f_y \\ f_z \end{pmatrix} = 0. \tag{3}$$

Here V represents the energy at the center of the gap and 2Δ the bulk band gap with the subscripts w and b denoting the appropriate values in the wells and barriers, respectively. The discontinuity in V is given by $V_b-V_w=(2Q-1)(\Delta_b-\Delta_w)$, where Q is the band-offset parameter and is defined as the fraction of the band-gap difference which lies in the conduction band.

The last three equations relate f_x, f_y, and f_z to f_s. By substituting them into the first equation, the set of equations is reduced to a single Schrödinger-like equation:

$$\frac{\hbar^2}{2l^2}\left[-\frac{d}{dz}\frac{1}{m(z,E)}\frac{d}{dz}+\frac{(z-k_y)^2+k_x^2}{m(z,E)}\right]f_s + [V(z)+\Delta(z)-E]f_s=0, \tag{4}$$

where now z and k_a are measured in units of l and $1/l$, respectively, and the renormalized mass is

$$m(z,E)=\hbar^2(E-V+\Delta)/2P^2. \tag{5}$$

In order to deduce the boundary conditions across an interface, we introduce a thin region at the interface in which the values of z-dependent functions are joined continuously. Integration of Eq. (4) across the interface and letting the thickness of the small interface region go to zero, yields the boundary conditions that f_s and

$$\frac{1}{m(z,E)}\frac{d}{dz}f_s$$

are both continuous.[1,3,4]

Since the magnetic subband states of interest in the CR measurements lie close to the bottom of the GaAs

well, we can carry out an expansion in terms of the parameter $\epsilon = E - V_w - \Delta_w$ which is the energy of the electron measured from the bottom of the GaAs well and can be treated as a small parameter in comparison to the energy gaps and conduction-band offsets. To leading order in ϵ,

$$m(z,E) = \begin{cases} m_w^* & \text{in the well,} \\ m_b = m_b^* - Q(m_b^* - m_w^*) & \text{in the barrier,} \end{cases} \quad (6)$$

where

$$m_{b,w}^* = \hbar^2 \Delta_{b,w} / P^2 \quad (7)$$

are the bulk masses.

As a result, the four-band $\mathbf{k}\cdot\mathbf{P}$ Hamiltonian is reduced to a one-band effective-mass equation with a renormalized effective mass. Notice that the renormalized mass is equal to the bulk effective mass in the wells but not in the barriers where the renormalized mass is dependent on the band-offset parameter Q. Using a value of $m_w^* = 0.067 m_e$ for the bulk effective mass in the GaAs well we obtain a renormalized mass $m_b^* = 0.09 m_e$ in the barrier, which is significantly reduced from the bulk band-edge AlAs barrier mass of $0.15 m_e$. Energy gaps of 1.52 eV for GaAs and 3.13 eV for AlAs with a band offset of $Q = 0.66$ were used in these estimates.[15] We have calculated the renormalized mass to the next order in ϵ and found the corrections to be about 3%. These higher-order results are not included in the analysis which follows.

Figure 2 shows the first five calculated magnetic energy levels as functions of the CR orbit center R_z, at $k_x = 0$ and for $B = 10$ T. Also shown is the $B = 0$ subband structure along k_z for reference. Note the strong dispersion which occurs in the higher-lying magnetic levels as they exceed the miniband width. Similar calculations performed for lower fields show no dispersion along the growth axis. This is in qualitative agreement with the experimental results discussed above. Figure 3 shows a quantitative comparison of the experimental CR absorption with the calculated transitions between the ground magnetic subband level and the first excited state as a function of field. At high fields (e.g., $B > 10$ T) the magnetic levels show strong dispersion along the growth axis and the greatly broadened experimental absorption line shape reflects contributions from transitions centered throughout the well and barrier. It has previously been shown that the dominant contribution to the tunneling CR absorption line shape is from the barrier bound transitions[12] where R_z is located inside a barrier. There is a sharp onset in the absorption spectrum at the barrier bound resonance frequency but convolution of the spectrum with a linewidth broadening function due to scattering and instrumental resolution moves the observed peak somewhat above the true absorption threshold. The theoretical results in Fig. 3 represent the transition energies at $R_z = 0$ and have not taken into account these linewidth broadening effects. Qualitatively, it is clear that if this shift were taken into account, the overall agreement would be substantially improved. Even without these corrections Fig. 3 clearly demonstrates that much better agreement with experiment is obtained by the renormalized effective-mass approach (EMA) rather than the one-band EMA.

Figure 3 also shows a comparison of the in-plane CR

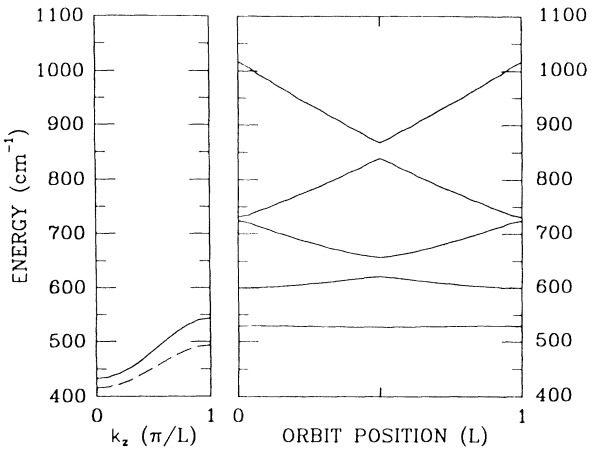

FIG. 2. The left panel shows the first subband at $B = 0$ and $k_x = 0, k_y = 0$. The solid line uses the renormalized barrier mass $m_b = 0.09 m_e$ and the dashed line uses the barrier band-edge effective mass $m_b^* = 0.15 m_e$. The right panel shows the first five levels at $B = 10$ T and $k_x = 0$ as functions of the position of the center of the CR orbit R_z. Here L denotes the period of the SL.

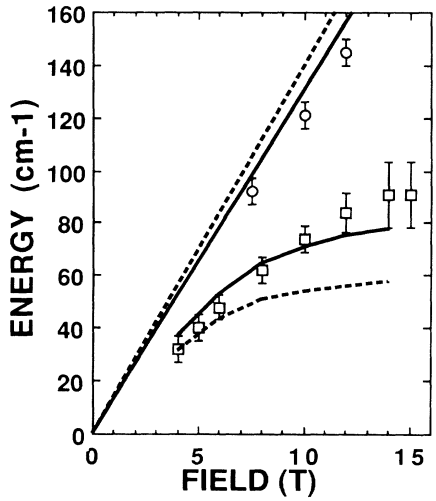

FIG. 3. A comparison of theoretical and experimental cyclotron energies with the field applied both parallel (circles) and perpendicular (squares) to the growth direction. The solid curves correspond to calculations using a renormalized effective mass. The dashed curves correspond to calculations involving the band-edge masses.

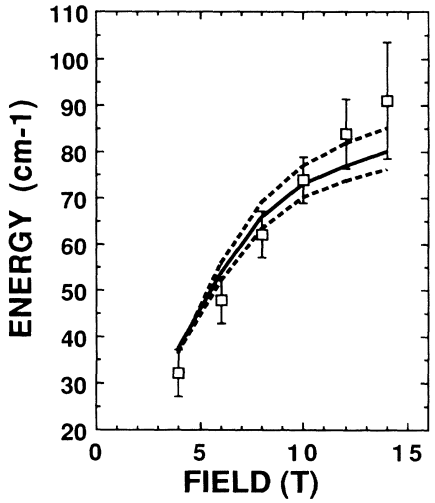

FIG. 4. Dependence of the calculated cyclotron energy on the barrier width at a fixed period of 84.4 Å. The solid curve corresponds to the measured barrier width of 10.5 Å and the top and bottom dashed curves to barriers of width 10.5 ± 0.6 Å, respectively, which reflects the experimental uncertainty. Note that this uncertainty is a small fraction of the thickness of a monolayer (2.8 Å).

measurements (e.g., B along the growth direction) with results obtained using the renormalized effective-mass approach. The correction to the classical in-plane CR mass was calculated to first order in ϵ yielding a value for the renormalized CR mass of $m^* = 0.072 m_e$ from the band-edge value $0.067 m_e$, and is seen from Fig. 3 to provide a better fit to the experimental data which yields a mass $m^* = 0.077 m_e$. It should be stressed that the mass enhancement calculated in this field configuration is *not due to nonparabolicity*, which is a second-order effect, but is due to the significant intrusion of the z component of the electron wave function into the AlAs barrier layers. Inclusion of nonparabolicity would further enhance the calculated mass and hence further improve the agreement with experiment.

The curves in Fig. 4 show the dependence of the cyclotron energy on the well width, L_w, and the barrier width, L_b, at constant period L. The dashed lines show the effect of increasing or decreasing the thickness of the barrier by $\frac{1}{4}$ *of a monolayer* (0.6 Å). The experiment and theoretical modeling are a demanding quantitative test of our understanding of tunneling through semiconductor barriers.

The renormalization of the mass deep in the band gap of semiconductor barriers is an important general result for quantitative descriptions of vertical transport in superlattices and heterostructures. This approach for theoretically handling the evanescent states deep in the band gap of barriers has kept the conceptual simplicity of a one-band effective-mass model and facilitates the design of artificial superlattice structures for new transport physics or new quantum transport devices. Tunneling cyclotron resonance has shown that this model gives a correct quantitative description of the tunneling rate in pure AlAs barriers.[6]

E. A. de Andrada e Silva would like to acknowledge support from Instituto de Pesquisas Espaciais, Sao Jose dos Campos–Sao Paulo, Brazil, for the leave of absence and partial financial support from Conselho Nacional de Desenvolimento Científico e Tecnológico. G. Brozak would like to thank Professor C. H. Perry for helpful discussions. The work at University of California, San Diego, is supported in part by NSF Grant No. DMR 88-5068. The work at Northeastern University is supported in part by NSF Grant No. DMR 8604706.

[1]D. J. Ben Daniel and C. B. Duke, Phys. Rev. **152**, 683 (1961).

[2]E. O. Kane, J. Phys. Chem. Solids **1**, 249 (1957).

[3]G. Bastard, Phys. Rev. B **25**, 7584 (1982).

[4]S. R. White and L. J. Sham, Phys. Rev. Lett. **47**, 879 (1981).

[5]K. J. Moore, G. Duggan, P. Dawson, and C. T. Foxon, Phys. Rev. B **38**, 5535 (1988).

[6]In an earlier effort (Ref. 7), a one-band effective-mass Hamiltonian (Ref. 10) was solved numerically where the experimental cyclotron resonance GaAs well mass $m^* = 0.077 m_e$ was used as an input parameter and where the AlAs barrier mass was varied in order to provide the best fit to the data; a value of $0.070 m_e$ was extracted for the tunneling mass. In the present approach we make no effort to fit theory to experiment but simply project the results of the four-band calculation onto the data. Given only the superlattice growth parameters, this model yields renormalized masses in both the wells and barriers. The tunneling masses which are obtained in these two approaches, although slightly different, are both consistently much lower than the band-edge mass $0.15 m_e$ which is now commonly used.

[7]G. Brozak, F. DeRosa, D. M. Hwang, P. Miceli, S. A. Schwarz, J. P. Harbison, L. T. Florez, and S. J. Allen, in Proceedings of the Eighth International Conference on the Electronic Properties of Two Dimensional Systems [Surf. Sci. (to be published)].

[8]S. A. Schwarz, C. L. Schwartz, J. P. Harbison, and L. T. Florez, in "SIMS VII" (Wiley, New York, to be published).

[9]T. Duffield, R. Bhat, M. Koza, D. M. Hwang, F. DeRosa, P. Grabbe, and S. J. Allen, Solid State Commun. **65**, 1483 (1988).

[10]J. C. Maan, Superlattices Microstruct. **2**, 557 (1986); Festkorperprobleme **27**, 137 (1987); G. Belle, J. C. Maan, and G. Weimann, Solid State Commun. **56**, 65 (1985).

[11]T. Duffield, R. Bhat, M. Koza, F. DeRosa, D. M. Hwang, P. Grabbe, and S. J. Allen, Phys. Rev. Lett. **56**, 2724 (1986).

[12]T. Duffield, R. Bhat, M. Koza, F. DeRosa, K. M. Rush, and S. J. Allen, Phys. Rev. Lett. **59**, 2693 (1987).

[13]Y.-T. Lu and L. J. Sham, Phys. Rev. B **40**, 5567 (1989).

[14]P. G. Harper, Proc. Phys. Soc. London A **58**, 879 (1955); J. Phys. Chem. Solids **82**, 495 (1957).

[15]O. Madelung, *Landolt-Bornstein: Numerical Data and Functional Relationships in Science and Technology* (Springer-Verlag, Berlin, 1987).